

© 2012 IEEE. Personal use of this material is permitted. Permission from IEEE must be obtained for all other uses, in any current or future media, including reprinting/republishing this material for advertising or promotional purposes, creating new collective works, for resale or redistribution to servers or lists, or reuse of any copyrighted component of this work in other works.

Sobh, Tarek M.; Mihali, Raul, "The Formula One Tire Changing Robot (F1-T.C.R.)," Proceedings of the 1999 IEEE International Conference on Robotics & Automation, Detroit, Michigan (May, 1999)

The Formula One Tire Changing Robot (F1-T.C.R.)

RAUL MIHALI and TAREK SOBH

Department of Computer Science and Engineering, University of Bridgeport, Bridgeport, CT 06601, USA

May 1998

Abstract:

Formula One racing is one of the most fascinating sports ever, it is a perfect combination of high speed, technology, pressure and danger.

One problem associated with car racing is the time differential between teams during pits stops, which substantially affects the final results. In addition, a high percentage of the accidents in Formula One is due to pit stop problems. Changing the tires of a car while almost in motion, after reaching dangerous pressure and temperature values, is a very risky challenge, no matter how well a team is trained. Approximately 15-25 people are constantly exposed to serious dangers. The risks taken are extreme and any idea of reducing it without affecting the quality of the race should be considered.

Our idea is to build a fully robotized system that takes over the tire changing and refueling process. There will practically be no need for human intervention. The system will demonstrate remarkable time accuracy, precision and low risk implications, uniformity of performance across teams, the competition being relayed solely upon the pilots.



Fig. 1. Car Model

1. Introduction

A high percentage of Formula One racing accidents occurs due to pit stop problems. Changing the tires of a car while almost in motion, after moving at speeds of 300 km/hour and reaching dangerous pressure and temperature values, is a very risky challenge for human beings, no matter how well trained they are.

In the following example, due to the malfunctioning of the refueling-equipment, the entire team including the pilot had to risk their lives; accident off the Benneton team, Joe Verstappen's car, 1994, Germany.



Fig. 2.a. Pit Stop accident (I)



Fig. 2.b. Pit Stop accident (II)



Fig. 2.c. Pit Stop accident (III)



Fig. 2.d. Pit Stop accident (IV)

A second problem of the pit stop is the considerable time difference between teams in the tire changing process. Suppose the team of the pilot currently on the second position can change the tires of their car in 8 seconds, while the team of the pilot from the pole position can do it only in 16 seconds. They usually do much better than that, however, today they seem not to coordinate that well. Such a difference will most probably change the position of the two pilots at the end of the race. While many fans consider it an exciting part of the race, it is not competitive at all because there is a great chance of not being able to keep such a time constant while working with 15-20 people. Even though this second problem of pit stops is a matter of taste, the high human risk implication still remains a key reason for a robotized solution. Watching a race with the idea that you might see fatal accidents while you clearly know that they can be avoided is unacceptable. The system presented here eliminates the presence of any team member around a car while in pits stop, assures an excellent quality of pit servicing and maintains the pit stop time constant, thus minimizing the risks on the pilot and improving the quality of the race.

1.1. PROBLEMS ENCOUNTERED / PERFORMANCE

In order to maintain the pit time low and constant, the first parameter to be optimized should be the *time accuracy*. More specifically, the robot has to change the tires of any car within the same time quantum. The current variance of *seconds* achieved by pit stop teams requires remarkable experience, but does not prove sufficient in a race, almost always affecting the final position of the pilots. A precision of 0.1 seconds or better between any two teams is required.

In the first version of our proposed system, a process length of 15 to 18 seconds will be achieved, and will be optimized to 6-8 seconds later.

Usually a pilot cannot stop easily in the pits with a precision of less than 5 centimeters or so. However, the manipulator needs it while working with the tires. Therefore, a sensor system will be implemented.

Another constraint is the *environment's limitations*. Only moderate changes in the pit stop's configuration can be allowed, due to the severe FIA regulations.

2. Brief Mechanical approach

2.1. PRAGMATIC CONSIDERATIONS/ ARMS REQUIRED/ WORKSPACE

Our proposed robotic system consists of 5 manipulators: one for each of the tires, and a fifth one for the fuel tank. To preserve the environment of the pit stop and to assure the comfort of the team we implement suspended manipulators. The support of the five arms (Figure 3) allows the sliding motion of each arm and also does not create any obstacles or driving difficulties for the pilot.

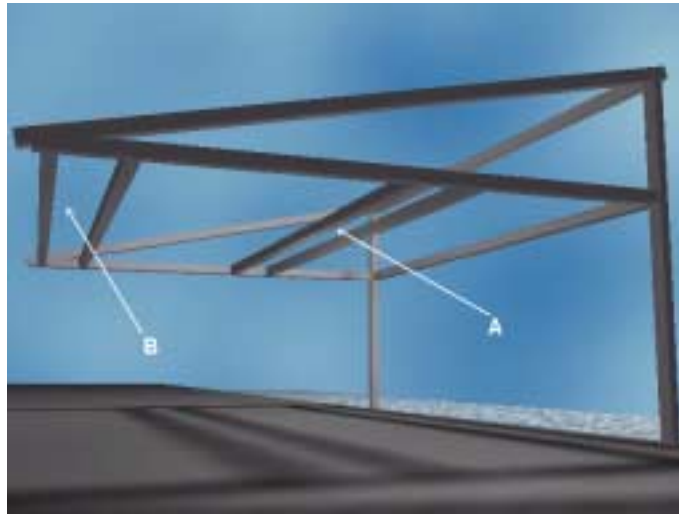


Fig. 3. View from the track side

The support has two double longitudinal branches on which the arms will be suspended, two arms on one pair of branches (sliding zone B), and three on the other one (sliding zone A). The sliding mechanism of the arms proves to be essential for the end effector positioning. The material has to be resistant, of low elasticity and capable of sustaining the mass of the arms. An extremely resistant and rigid material needs to be used.



Fig. 4. Typical Formula One Car

Because a wheel of a Formula One car is attached with a single central screw (See Figure 5), there is design space for a flexible end - effector, with less required torque and mass. The multi screw wheels from streetcars would complicate significantly the system, a different version of this robot is currently being considered for that purpose too.

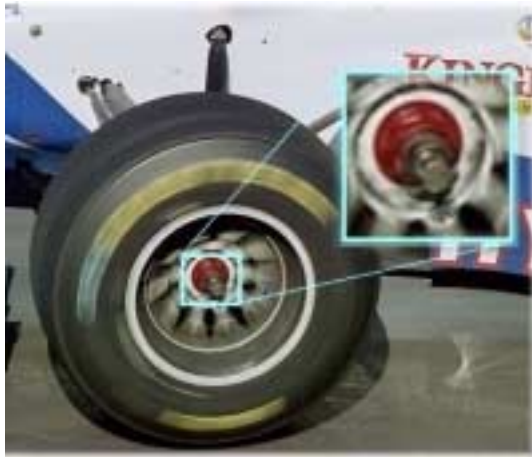


Fig. 5. Tire close-up



Fig. 6. Tire CAD Design

Figure 5 shows a close-up of the “one screw” tire and figure 6 shows a CAD design of a tire as it will be displayed after the sensor system interprets the position of the four wheel holes.

Each of the manipulators has a sliding range of (1 -1.5 meters on the supports and can handle a tire in many ways. The only plane in which a good dexterity is required is the horizontal one, due to the fact that the distance from the ground and the tire’s central axis is relatively constant (a certain tolerance will be assumed). Based on the above-mentioned requirements, the manipulator design in Figures 7, 8, 9 has been reached.

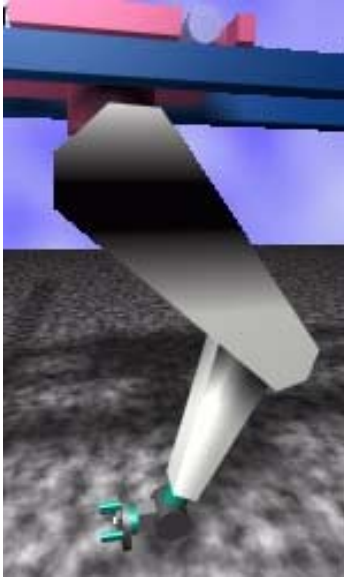


Fig. 7. Side view

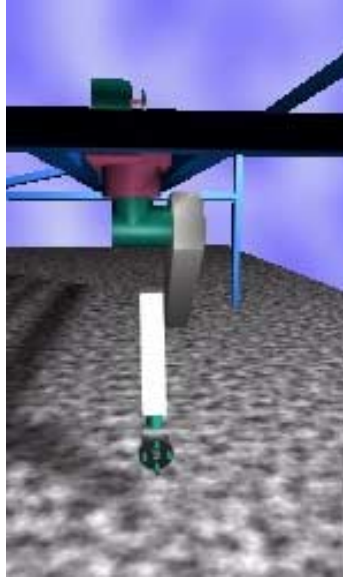


Fig. 8. Front view

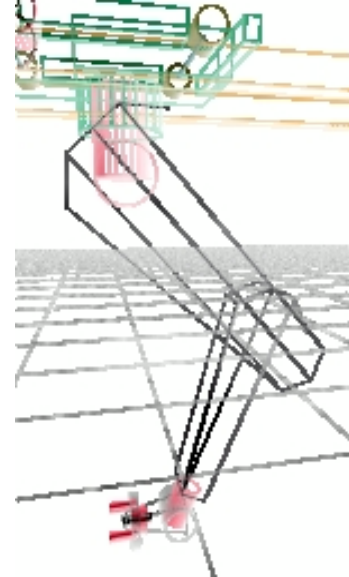


Fig. 9. Wire-frame side view

2.2. TASKS AND MOTION RELATED BRIEFINGS

The car arrives into the pits from a certain direction and stops in approximately the same position every time. By the time the car arrives, the robot's sensor system registers it and notes the exact position and direction of the tires. Once the car stops, the arms start the *tire changing process*. For lifting the car, a simple lifting system will be implemented and positioned on the stopping platform, which would suspend the car throughout the whole process. Each tire handling manipulator has to go through the following task sequence:

- ⇒ Position the end effector as a function of the tire parameters received from the sensor system
- ⇒ Rotate the end effector so that it can catch the tire
- ⇒ Grab the tire
- ⇒ Remove the screw
- ⇒ Remove the tire from its axis and put it on the ground near the car in a convenient spot
- ⇒ Change the position and grab the new tire, located in the proximity, with a new screw on it
- ⇒ Position again the end effector and fix the new tire on the axis
- ⇒ Tighten the screw
- ⇒ Move back in the *stand-by* position to enable the car's departure.

There are about 15 different moves to be done, each one in about 1 second, which would allow a process length of approximately 15 seconds per manipulator. Of course all the arms work in parallel and independently.

The positioning of the end effector and actually the entire set of movements required are of short distance and mainly consist of revolute steps: arm expansion / contraction, arm / end effector rotation and end effector positioning. There is a good probability that the specified time of one second per move can be reduced.

Four micro sensors will be mounted on each tire, responsible for specifying the tire's angle and position relative to the arm. According to the information from these sensors, the end effector can position itself perpendicularly on the tire and grab it correctly. We didn't have yet the chance to work on a racecar, but the system can be easily adjusted in case the dimensions vary a bit from the one we considered.

The rotation of the screw is a simple task, implying the activation of one compressed air tool located in the end effector.

The most time consuming task is handling of the tire itself. This task requires good torque and acceleration control on the entire arm, implying the activation of all the engines, including precision sliding. The time interval from removing the old tire and replacing it with the new one it is estimated to be approximately 3-5 seconds. A team member will position the replacement tires in the proximity of each arm before the car would arrive in the pits

Moving back in the stand-by position is again a simple task and can be completed partially when the car leaves. As long as the arms are at a safe distance from the tires the car can be ready to go.

Because of the sliding mechanism, the pilot can allow errors of up to half a meter while parking. However, there are still some exceptional positions, which will require special attention.

2.3. JOINT / LINK REQUIREMENTS AND CONSTRUCTION

One arm is composed of 4 joints and the end effector. The first joint is a prismatic one, constituted by the sliding part of the system, as shown in figures 10 and 11.

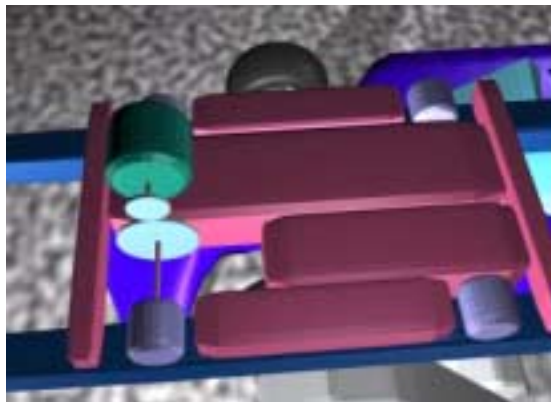


Fig. 10. The slider (top)



Fig. 11. The slider (beneath)

Figures 10 and 11 depict a sketch of the actual mechanism, a view from the top of the robot with the car behind on the left and on a general view from beneath the arm on the right taken from the car's side, driver's position. The prismatic movement is controlled by one motor fixed as shown. The torque/mass ratio of the motor does not have to be stringent, and a sliding accuracy of 1mm should be sufficient. Typically, the slider is activated just in the beginning of the full tire changing process, in order to fix the arm in an appropriate position. The friction coefficient of sliding between the support and the four wheels has to allow a stable braking with a precision of 1m/s^2 and the friction coefficient of revolution has to allow low acceleration control.

The joint has a braking mechanism (not visible in the figure) which activates once the requested position has been achieved. This will simply lock the arm on the support while changing the tire, thus reducing the resultant of the vertical and horizontal vibrations. All arm motors work at high speed, have significant mass, and so the inertia problem has to be considered carefully ([5, 7, 11]).

Controlling this joint is the easiest task as long as it does not have to be part of the robot's equations. To use time optimally, the arm will move - from /to - the stand-by position - to /from - the ready position in the same time with the sliding action (more details in the *Controlling* and *Parameters* related sections).

The second joint is a revolute one, as are all of the following ones. The next four figures (12-15) show the joint and indicate the rotation direction. The view is from the bottom left of the joint (car side) in Figures 12 / 14 and the view is from above, right side on Figures 13 / 15 - Phong and wireframe views.



Fig. 12. Second joint view I

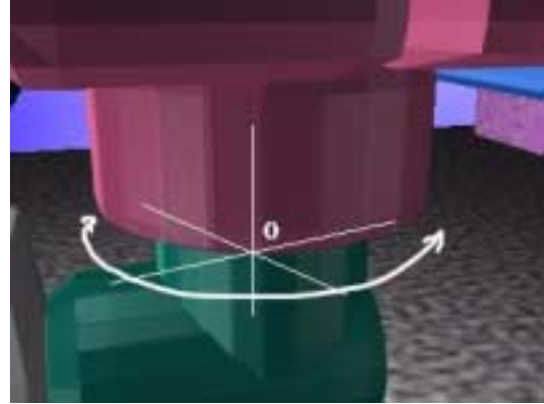


Fig. 13. Second joint view II

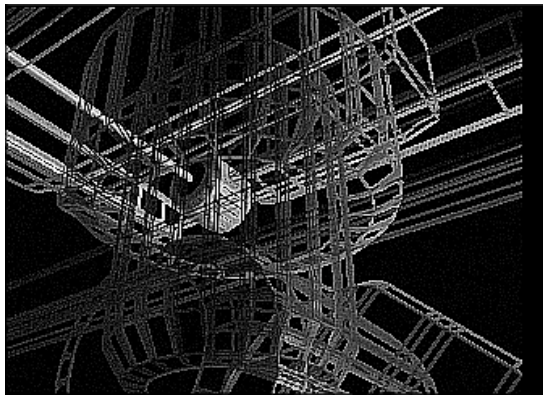


Fig. 14. Second joint view I (wire-frame)

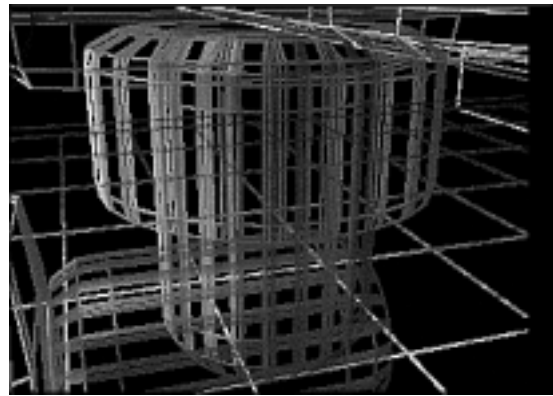


Fig. 15. Second joint view II (wire-frame)

The second joint is an essential orientation joint and is controlled by a strong motor, because it supports most of the tensions of the other motors and masses. A revolution limitation of $3/2 * \pi$ might seem subjective, but limiting it does not create kinetic or dynamic problems (e.g. singularities). The motor is fixed in the sliding part, thus allowing flexibility in mass, the pressure now being moved on the normals between the support and the 4 wheels of each slider.

The third joint is closely mounted near the previous one, and together with it and the sliding joint forms the *static* main concentration of mass and torque of the arm. Figures 16, 18 show the view from the car's side, under the slider and Figures 17, 19 show the view from the arm side on the right.

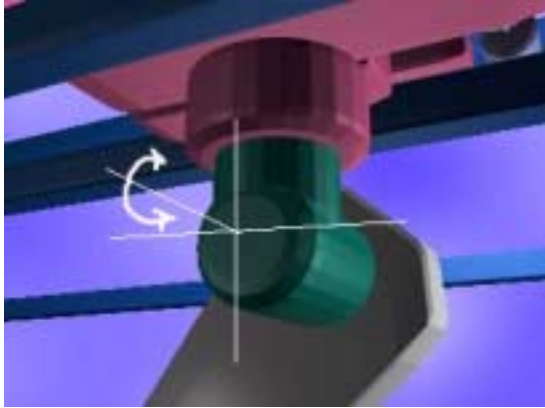


Fig. 16. Third joint view I

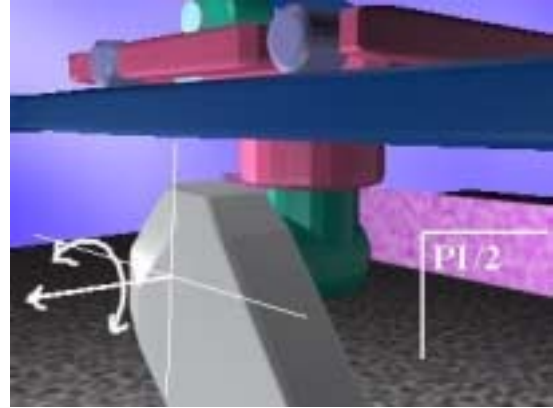


Fig. 17. Third joint view II

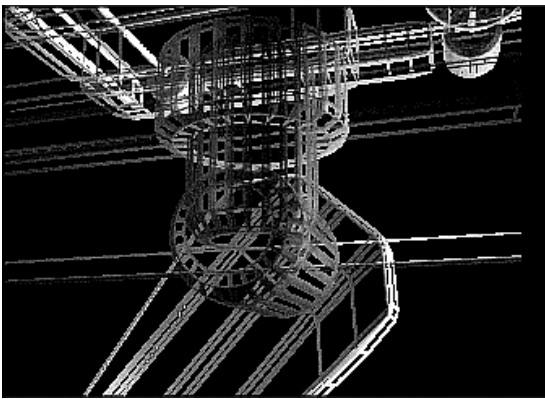


Fig. 18. Third joint view I (wire-frame)

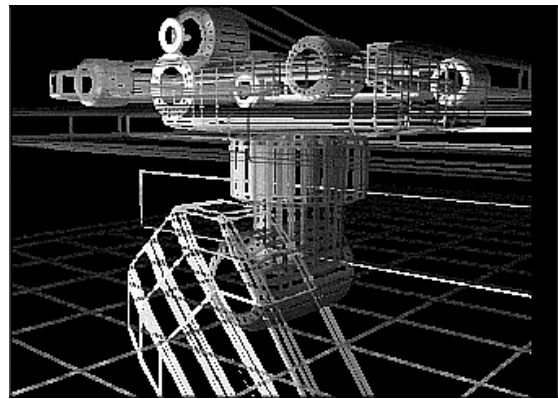


Fig. 19. Third joint view II (wire-frame)

It is necessary to keep a high torque in this part of the arm, to allow a better torque control for the next joints while a tire is being manipulated. Thus, the motor of this joint has to be attached to the axis of the previous joint, which will remain locked while manipulating the tire. The remainder of the arm has to be as light as possible because it forms the *transportable* part of it (due to the fact that it will be the only one moving once the static part finishes its task). The angle of rotation has been limited to less than $\pi/2$ degrees (singularity reasons).

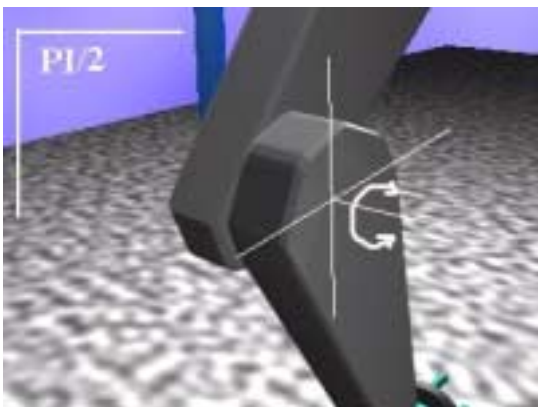


Fig. 20. Elbow joint view I



Fig. 21. Elbow joint view II

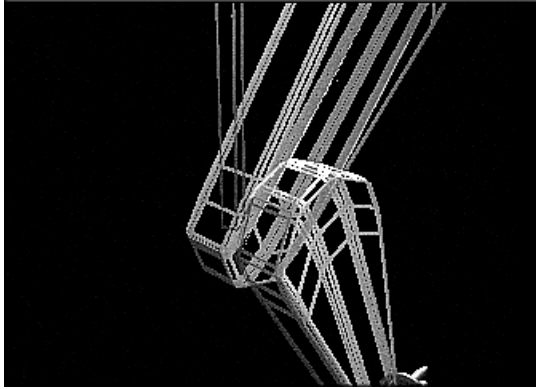


Fig. 22. Elbow joint view I (wire-frame)

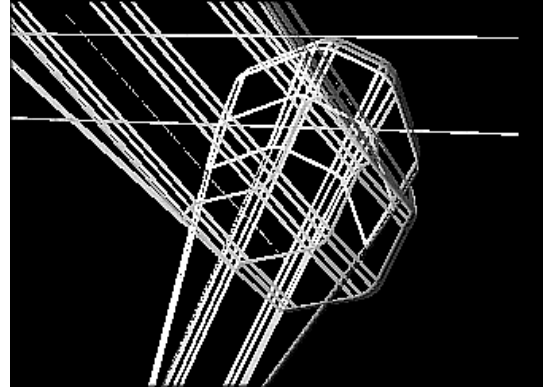


Fig. 23. Elbow joint view II (wire-frame)

The last revolute joint from the arm segment is the elbow joint (Shown in figures 20-23). This joint's motor should be light and has a relatively small torque. The transportable part of the arm has to be as light as possible in order to achieving the required speed and torque. It is installed in the upper part of the arm, thus keeping a safe distribution of mass. The angle of revolution has been limited to no more than $\pi/2$ degree again. This range fits the requested tasks and also does not create singularities.

The pressure should be as small as possible on the contacts between the support and the arms, especially while the five arms work together and the vibrations in the support are high, forcing a dislocation. The critical positions of the arm are the *stand-by* one and the *fully extended* one, as shown in figures 24 and 25.

Fig. 24. *Stand-by* positionFig. 25. *Fully extended* position

The stand-by position is safe enough to offer the pilot a good visibility while entering the pits. The dimensions of the links will be specified later in the presentation. As an example the car does not exceed 1m in height and the slider of the arm is situated at about 2m above the ground.

2.4.THE END EFFECTOR (DESIGN /JOINTS/ DEXTERITY/ POWER/ ACCURACY)

The end effector has to be small and light, but powerful, dexterous and quick. In the early stages of the design, we opted for a double-ended effector design. This would have allowed a faster manipulation of the tires because it would not require the arm to put the tire down and grab the new one. The arm would get loaded with the new tire at one of the sides of the effector, the one opposite to the car. When the car would stop, the other side of the effector would remove the screw and grab the used tire, then do a π degree rotation on the central vertical axis and attach the new tire to the car body.

After calculating the required dimensions and torque for the materials and engines, the results were discouraging, the required torque being not realistic. Another problem that became apparent was the high vibration in the entire system. Once the end effector would spin, a helicoidal path of motion would get employed, resulting in strong moments tending to dislocate the arm from the support, pulling it up.

After trying few more designs, we stopped at the one from Figure 29. This is a single ended-effector, a change that was necessary, to avoid the high forces from the supports.

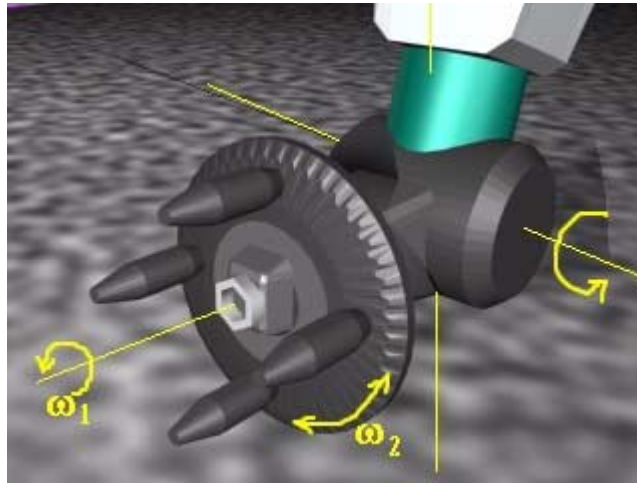


Fig. 29. End effector (final design)

This model solved all the problems so far. First, there are no more positioning problems. The disk type effector can rotate at a speed ω_2 , and reach any orientation requested by the sensor system. Having four identical tools, there would not be any more equilibrium problems during transportation. The electro-magnetic forces are well distributed now and allow movements within a wide acceleration range.

The revolute joint between the arm and the effector allows a rotation in the vertical plane of $\pi/2$ degrees. The motor is installed in the cylinder in order to allow for uniform mass distribution in the entire arm. The motor that spins the disk with the four side segments is installed in the pyramidal body following the cylinder. In the same spot the compressed-air system is installed (for screw-removal).

The only rotation that cannot be performed by this end effector is the one on the vertical axis. This one, however, it is covered by the first revolute joint at the base of the arm, which supports most of the torque and allows for good acceleration control. So at this point the end effector is able to operate for almost any reachable position of the tire. Another advantage of this arm style is that the tire doesn't have to be perpendicular to the ground (supposing an accident has happened). The end effector would still be able to accommodate the correct orientation. However, once the tire isn't perpendicular to the ground this would mean that the car has been damaged seriously and most probably needs intervention of the team (another advantage of mounting sensor in the tires).

Another issue to be clarified is the way in which the compressed air screwdriver finds the position of the screws: The screw driver starts a revolute task and at the same time tries to advance slowly until it "fits" the faces of the screw and fixes onto the screw.

The arm without the end effector, the sliding mechanism and its very rigid structure requirements, it is very similar to the PUMA 560 arm series ([9, 12, 19]) and we are considering to refurbish a PUMA arm for testing purpose.

3. Direct and inverse Kinematics approach

One of the next steps is solving the direct and inverse kinematics for this specific manipulator (Figure 30).

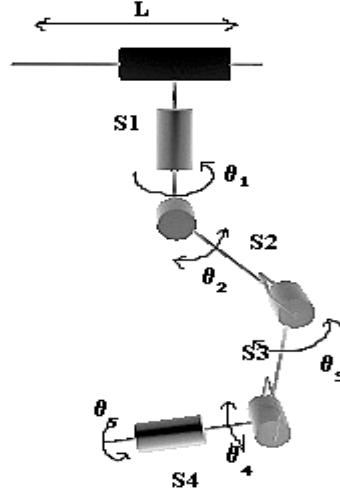


Fig. 30. Manipulator scheme A

Here, 6 joints of the arm can be seen. Using the Denavit-Hartenberg table [2], the equations for the direct kinematics can be written as (the dimensions of the links are known):

$$X = L + \cos(\theta_1) * (S2 * \sin(\theta_2) - S3 * \sin(\theta_2 + \theta_3) - S4 * \sin(\theta_2 + \theta_3 + \theta_4 - \pi))$$

$$Y = -\sin(\theta_1) * (S2 * \sin(\theta_2) - S3 * \sin(\theta_2 + \theta_3) - S4 * \sin(\theta_2 + \theta_3 + \theta_4 - \pi))$$

$$Z = S1 + S2 * \cos(\theta_2) - S3 * \cos(\theta_2 + \theta_3) - S4 * \cos(\theta_2 + \theta_3 + \theta_4 - \pi)$$

$$\theta_x = 0$$

$$\theta_y = 3\pi/2 - (\theta_2 + \theta_3 + \theta_4)$$

$$\theta_z = \theta_1$$

Where X, Y, Z, are the coordinates and θ_x , θ_y , θ_z the orientations of the end effector.

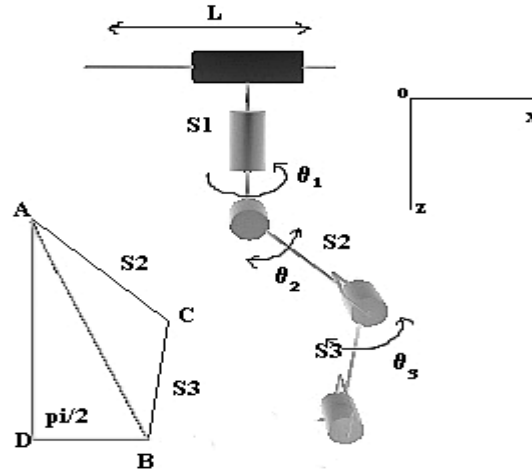


Fig. 31. Manipulator scheme B

Solving for the inverse kinematics using direct algebraic methods [18], we obtain the following model:

$$L = (Y / \tan(\theta_z))$$

$$\theta_1 = \theta_z$$

$$\theta_3 = \arccos((S2 * S2 + S3 * S3 - (X + S4 * \sin(\pi/2 - \theta_y) * \cos(\theta_z) - (Y / \tan(\theta_z))) * (X + S4 * \sin(\pi/2 - \theta_y) * \cos(\theta_z) - (Y / \tan(\theta_z))) - (Z + S4 * \cos(\pi/2 - \theta_y) - S1) * (Z + S4 * \cos(\pi/2 - \theta_y) - S1)) / (2 * S2 * S3))$$

$$\theta_2 = \arccos((- (S3 * \sin(\theta_3)) * ((X - (Y / \tan(\theta_z))) / \cos(\theta_1) + S4 * \sin(\pi/2 - \theta_y)) + (S2 - S3 * \cos(\theta_3)) * \sqrt{(S2 - S3 * \cos(\theta_3)) * (S2 - S3 * \cos(\theta_3)) + (S3 * \sin(\theta_3)) * (S3 * \sin(\theta_3)) - ((X - (Y / \tan(\theta_z))) / \cos(\theta_1) + S4 * \sin(\pi/2 - \theta_y)) * ((X - (Y / \tan(\theta_z))) / \cos(\theta_1) + S4 * \sin(\pi/2 - \theta_y))} / ((S2 - S3 * \cos(\theta_3)) * (S2 - S3 * \cos(\theta_3)) + (S3 * \sin(\theta_3)) * (S3 * \sin(\theta_3))))$$

$$\theta_4 = 3 * \pi/2 - \theta_y - \theta_2 - \theta_3$$

Figure (31) proves to be helpful when describing the position and orientation of the end effector in terms of the tire's coordinates, obtained from the sensor system.

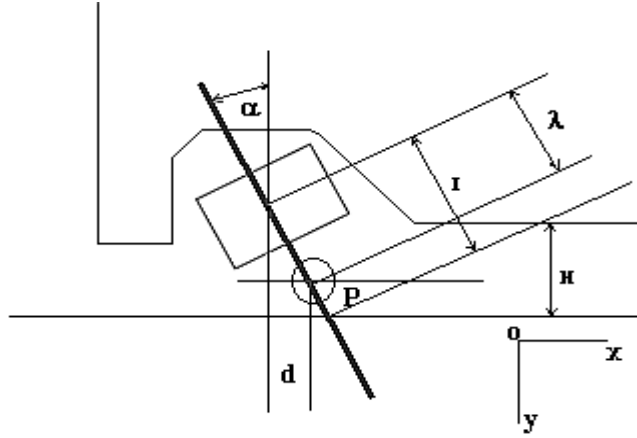


Fig. 32. Front left tire scheme (top)

The metrics referred to are as shown in figure (32):

α = The angle between the tire and the normal to the slider

P = The position of the end effector

H = The distance between the slider and the car

I = The distance from the center of the tire to the center of the slider

λ = The distance from the center of the tire to the position of the end effector

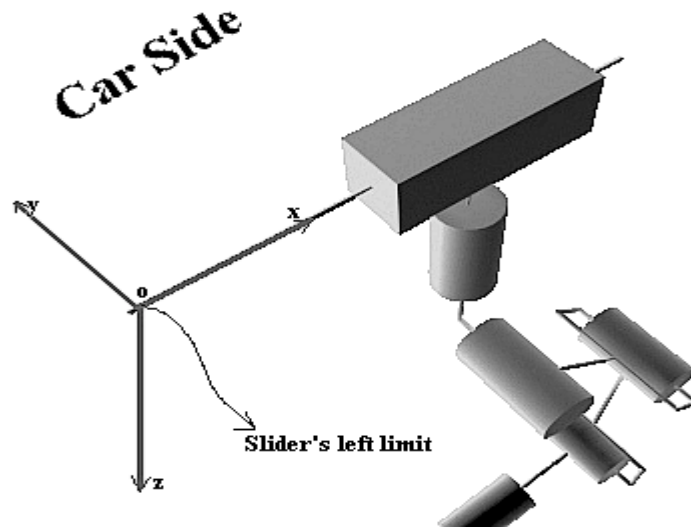


Fig. 33. The slider

The origin of XYZO is situated at the left end of the slider and so we have a positive moving distance. The positions of the tire are referred by the sensor system to the same XYZO. Specific dimensions for the lengths and other metrics are available in the software package.

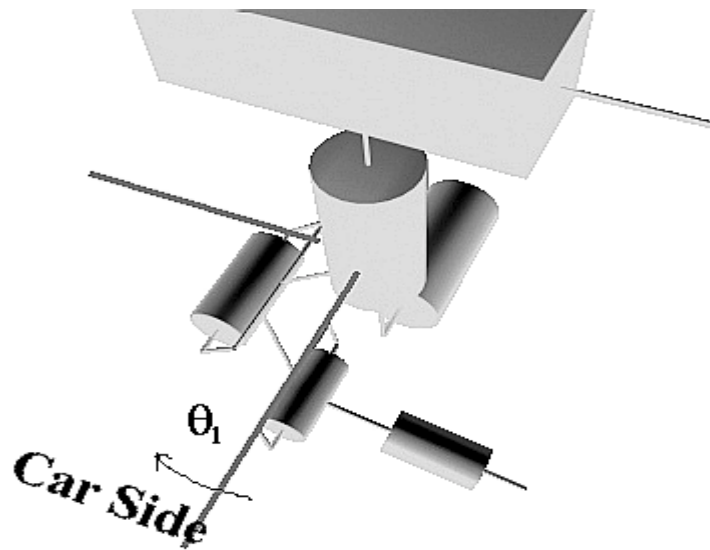


Fig. 34. Second joint.

For the first joint the angle doesn't have to exceed PI degrees (See figure 34). As initial position (or stand-by), the angle will be always positioned at 0 degrees. The following 3 joints have been referred in terms of the previous link direction.

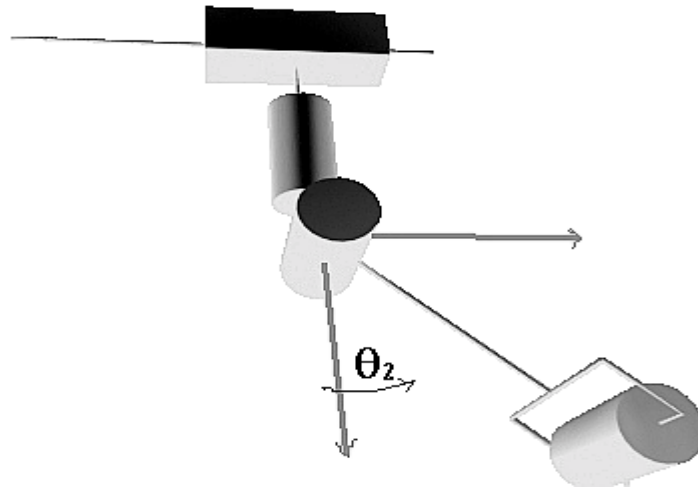


Fig. 35. Third joint

For joint 2 (figure 35) the angle doesn't have to exceed $\pi/2$. The angle will reach a value close to 0 degree very rarely (when the car is situated further away from the arm, about 80cm or more). The initial position of this angle will be set close to $\pi/2$, so the link will go up.

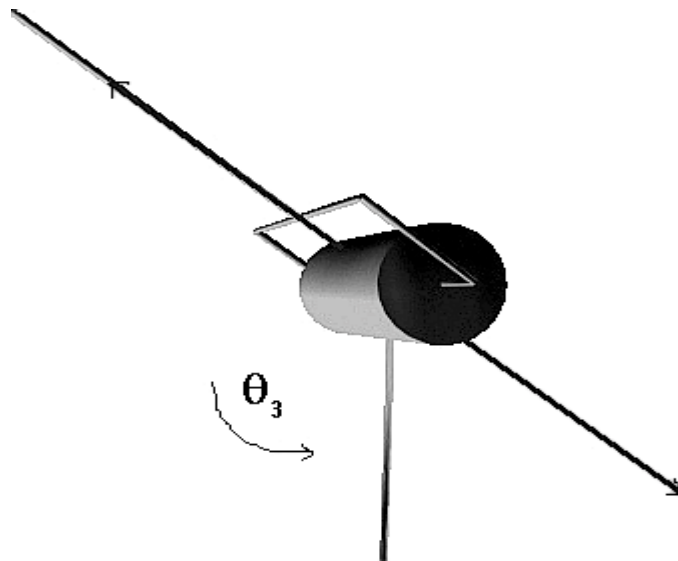


Fig. 36. Elbow joint

For joint 3 (figure 36), the reference to the previous link proves a superfluous allowance for the angle, because the architecture of the robot does not allow angles less than $\pi/12$. So we use values between $\pi/12$ and up to π . For the stand-by position the angle will be set around $\pi/12$.

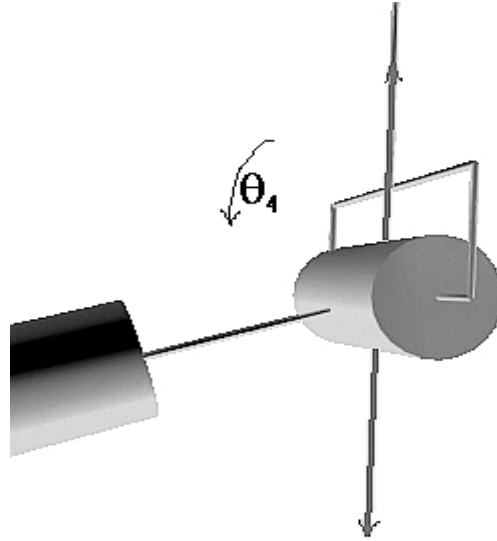


Fig. 37. Fourth joint.

Joint 4 (figure 37) has lower limits than physically possible. The angle value shouldn't be smaller than $\pi / 4$ and also no bigger than $5 * \pi / 4$. Very small angles simply can't be reached - because of the architecture of the arm. Slightly larger angles (close to $\pi / 4$ or $5 * \pi / 4$) would cause problems holding the tire. A value of $\pi / 2$ is used for the stand-by position and also for the P position - Figure 32.

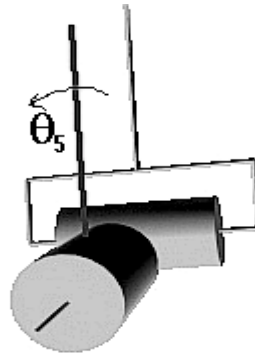


Fig. 38. Fifth joint

The final joint (figure 38) is adjusted independently from the others. The rotation direction matters as regards to controlling the torque. The value can run from 0 up to $2 * \pi$. A software tracking system is being built, allowing rotating the 4 segments synchronously from the moment the sensor system gives information about the tire's position. Thus, the angle can go up to $n * \pi$. This might be useful when the achieved speed is not satisfactory and there is a need to position the tools in advance.

For velocity and acceleration kinematics, the equations obtained from the D-H table define a function between the Cartesian space of positions and directions and the joint positions. We determine the velocity derivating the Jacobean of this function. Decoupling of singularities is not necessary as long as the design allows the avoidance of these.

The inverse velocity and acceleration are obtained from the following derivations:

$$\dot{\mathbf{q}} = \mathbf{J}(\mathbf{q})^{-1} * \dot{\mathbf{X}}$$

$$\ddot{\mathbf{q}} = \mathbf{J}(\mathbf{q})^{-1} * \mathbf{b}$$

Where

$$\mathbf{b} = \ddot{\mathbf{X}} - \frac{d}{dt} * \mathbf{J}(\mathbf{q}) * \dot{\mathbf{q}}$$

$$\ddot{\mathbf{X}} = \mathbf{J}(\mathbf{q}) * \ddot{\mathbf{q}} + \frac{d}{dt} * \mathbf{J}(\mathbf{q}) * \dot{\mathbf{q}}$$

Where:

\mathbf{q} = the vector of joint coordinates;

$\mathbf{J}(\mathbf{q}), \mathbf{J}(\mathbf{q})^{-1}$ = the Jacobian and inverse Jacobian of \mathbf{q}

\mathbf{X} = the vector of end effector coordinates

4. Direct and inverse dynamics approach

For this type of arm the following dynamics model ([1, 2, 4, 5, 6]) is used:

$$\boldsymbol{\tau} = \mathbf{M}(\mathbf{q})\ddot{\mathbf{q}} + \mathbf{V}(\mathbf{q}, \dot{\mathbf{q}}) + \mathbf{G}(\mathbf{q}) + \mathbf{F}(\mathbf{q}, \dot{\mathbf{q}})$$

$$\ddot{\mathbf{q}} = \mathbf{M}^{-1}(\mathbf{q})[\boldsymbol{\tau} - \mathbf{V}(\mathbf{q}, \dot{\mathbf{q}}) - \mathbf{G}(\mathbf{q}) - \mathbf{F}(\mathbf{q}, \dot{\mathbf{q}})]$$

Where:

$\boldsymbol{\tau}$ = the end effector torque,

\mathbf{M} = the symmetric joint-space inertia matrix,

\mathbf{V} = describes *Coriolis* and *centripetal* effects [2,6,7],

\mathbf{G} = the gravity loading,

\mathbf{F} = the end effector force.

5. The Sensor System. Implementation and Sensing

The variable elements derived from the sensor system that participated in computing the inverse kinematics equations were Cx, Cy and the angle α made by the tire's axis with the slider (as shown in Figures 39-40). These parameters are required for each tire, so there is a need for four sensor sensing systems. Furthermore, we also need the XYZ coordinates of each of the four tire holes. Once we acquire the coordinates of the four holes of one tire, the other variables can be easily deducted, as long as Cx and Cy represent the center of the parallelepiped made by the holes' position and then translated with a constant k representing the width of the tire.

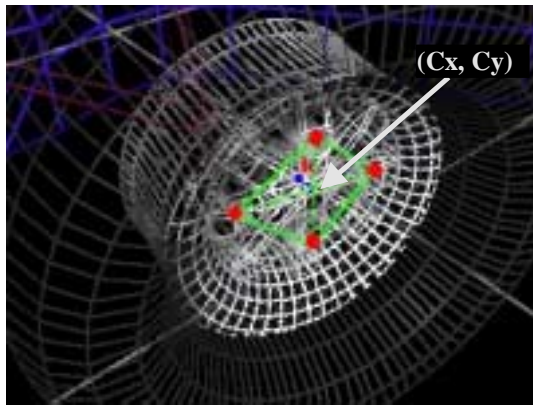


Fig. 39. Front left tire (wire-frame close-up)

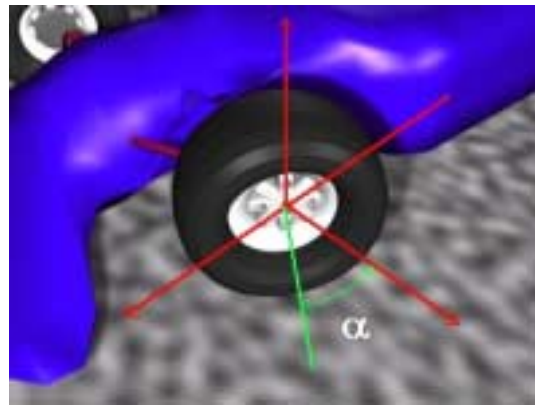


Fig. 40. Front left tire (shaded view)

The data that has to be supplied by the sensor system consists of the tri-dimensional coordinates of 16 points (for each tire there are four holes that need to be located). The angle between the axis of the front and rear tires is α . The rear tires will never change the angle relative to the rest of the car. The front tires are parallel, otherwise the car would have serious damages. The tires are always referable to each other, as long as the distance between them is constant (having a variable distance between the tires would result in abnormal situations).

Once we obtain the positions of one of the front tire's holes and one of the rear tires' holes, we can build easily the other coordinates required. Figure 41 depicts the variable angle between the axis of the front and rear tires.

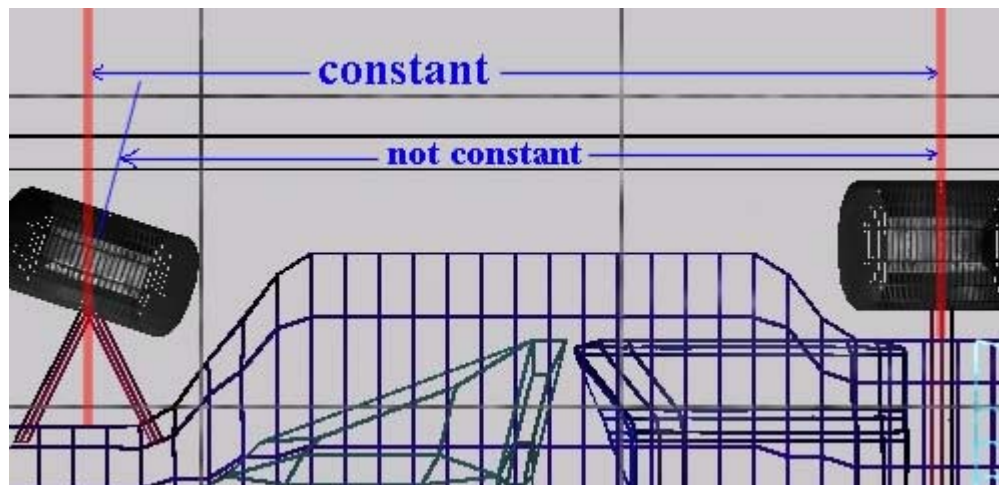


Fig. 41. The car (view from above – wire-frame)

5.1. MOTION ACCURACY

There is a need to control the number of times per second the sensor system provides data ([18, 19]). This is important to determine the car's motion. Motion recovery would allow one arm to track the tire and to have the end - effector positioned even before the car would stop, thus gaining some time. In case the software kinematics solution is slow in real time, a hardware implementation has to be taken in consideration.

5.2 TECHNOLOGICAL ORIENTATION

According to the required sensor system tasks, one of possible implementations for this sensory system can be through a radio radar detector ([13, 14, 17]).

Using video cam systems would complicate the problem because of the high-detail image processing that would be required. There are already built sensor system with accuracy close to our needs, but they prove to be too expensive and resource consuming [15, 16, 17]. We could also choose a laser scanning system and further complicate the interpretation of the data. So long as four micro sensors can be installed on the tires, the problem becomes more manageable.

The scanning part of the system situated somewhere close to the scene, would always stay in a scan mode and pick signals from the tires.

The sensors of the tires will be scanned send every tenth of a second. Once the scanner reads the sensors, this implies that the car is situated somewhere close to the pits and according to the distance and the speed of the car the software will process and send the necessary information to the arm controller. Note that the weather condition or other external factors are of minimal effect on this sensing system.

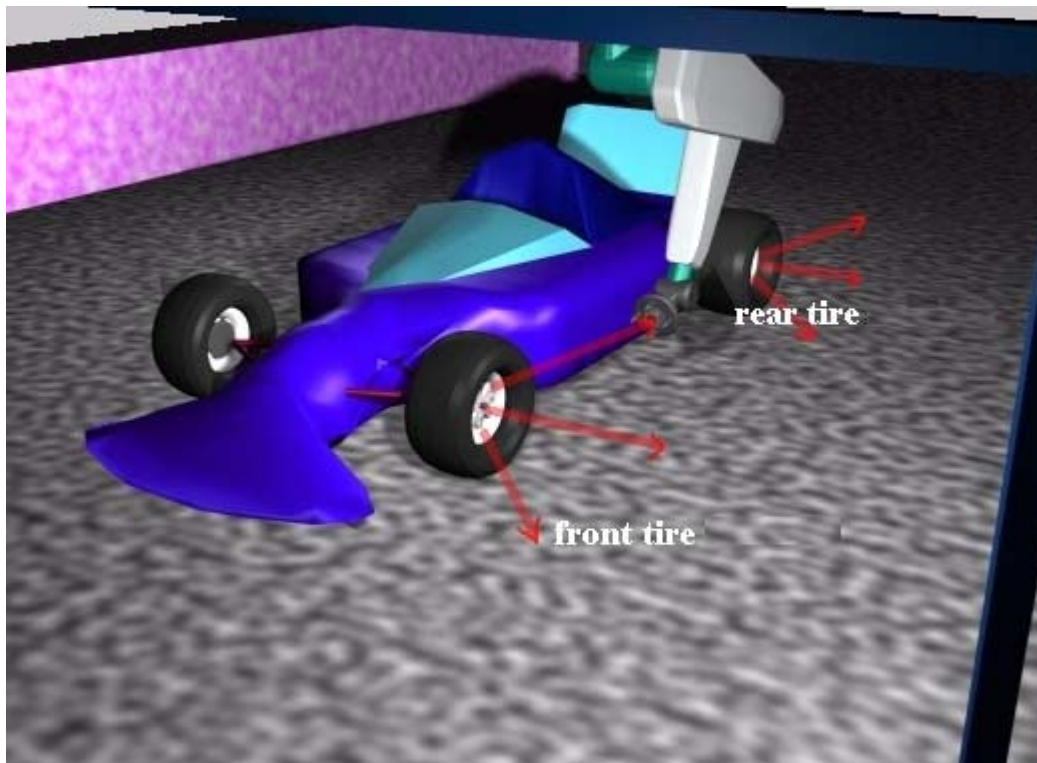


Fig. 42. Sensor locations

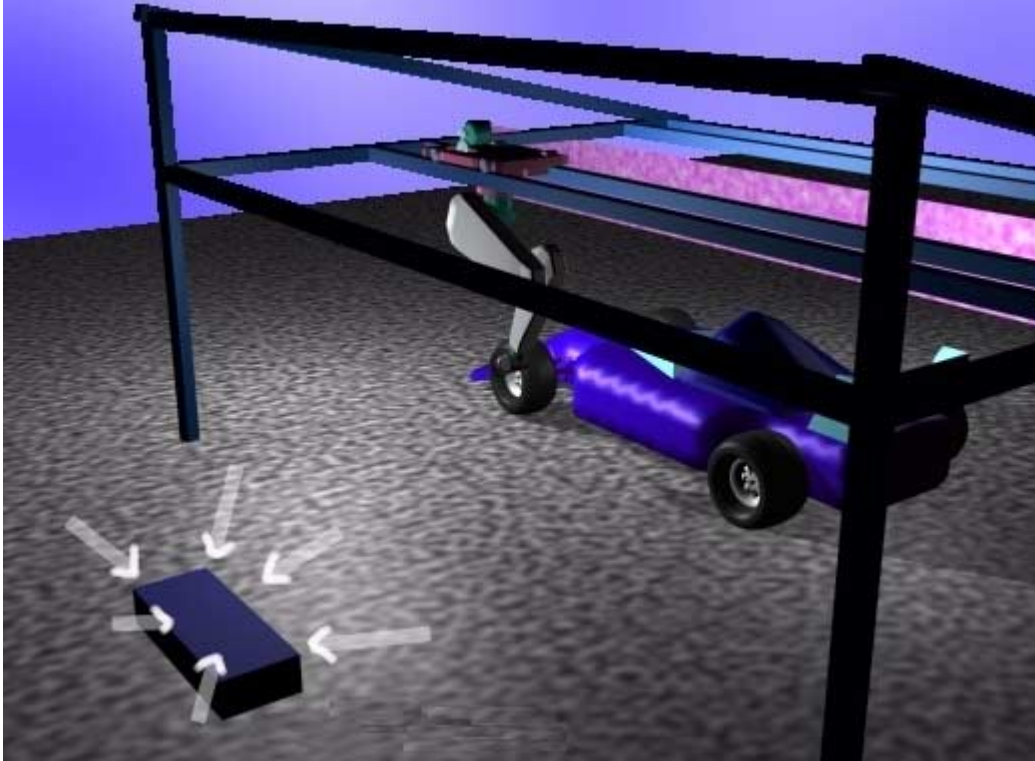


Fig. 43. Scanning point

The scanner could get data from the tires each time the car passes near the pits. The skew of the tires can be calculated simply from one frame and represents an extension in 3D of the angle α . For the oscillations we need more frames so that the distance between the ground and tire can be analyzed. This vertical distance Δy can be calculated from two frames having holes at about the same orientation ω (please refer to the *Direct and Inverse Kinematics* section).

For horizontal displacements, it is necessary to add some sensors on the tires from the other side of the car. Other tasks could be assigned to this system (i. e. analyzing the information from all the four tires, scanning the planarity of the car, vibrations, installation of new sensors providing different types of information, etc).

6. Controlling and supervising

The system will work perfectly for at least a couple of hours, more exactly it will be able to handle up to 5 tire changing sessions per car during a race, without any technical assistance needed. In order to assure this quality, supervising and controlling will be done from a control room located in the proximity of the pits.

6.1. TASKS IMPLIED

We need to be able to analyze at any moment the following parameters:

- ⇒ For each engine manipulator, response per input power, activation requests and discrepancy between request and reply, internal functionality status

- ⇒ joint position and orientation, difference between requested revolution angle and the resulting one, smoothness of revolution, response time delay
- ⇒ link position and orientation, difference between requested and resulting position, synchronization with the joints
- ⇒ mass distribution in each arm, vibration factor evolution
- ⇒ sensor system supervising:
 - evolution of the delay in answering
 - discrepancy between the detected position of the holes and the real one deducted from the final correction of the end effector
 - internal functionality status
- ⇒ tire sensors displacement in time, sensor functionality and reply frequency
- ⇒ support displacement and internal tension during arms motions, vibration and material response
- ⇒ temperature and pressure of the environment, wind velocity and direction as well as temperature evolution for each of the engine
- ⇒ parameter analysis evolution and general system status

The required joints positions and orientations will be always pre-simulated and compared with the ones obtained from the direct sensor output. The parameter differences will be corrected using mostly PID control.

We implement digital feedback controllers for the system using a proportional plus derivative (PD) control ([10,17,19]), simplifying considerably the nonlinear dynamic equations, but also requiring a high update rate. We use a dynamic model for the simulation and control (Figure 44). To avoid jamming due to collision with other objects or parts, impedance control algorithms are to be considered too.

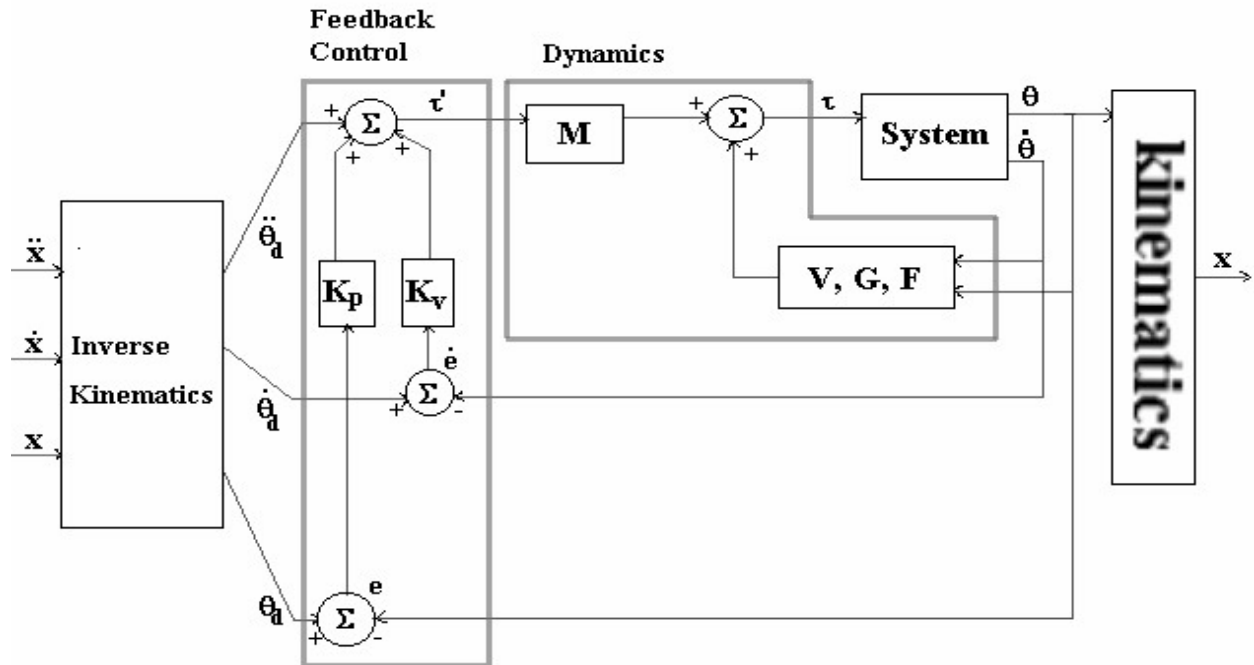


Fig. 44.

6.2. FLEXIBLE PARAMETER ANALYSIS

The data received from the sensing board of each arm has to be interpreted and displayed. Most of the parameters have to be shown graphically and forecasting functions have to be used. Good proximity forecasting functions [15, 16] will help a lot in the identification of recoverable damages.

Normally one of the controlling stations will display a real time recording of the coordinated arm, a simulation view showing the requested motion, actual position and simulated response of the arm

6.3. CURRENT DEVELOPMENT STAGE & RESULTS

Currently the robot CAD module is functional and is connected with the kinematics and dynamics modules. Animation and simulations showing the entire tire changing process has been done too. The following example (figure 45) shows graphically the torque that has to be applied on three joints for a full extension of the arm from a fully compressed position, considering a time frame of one second.

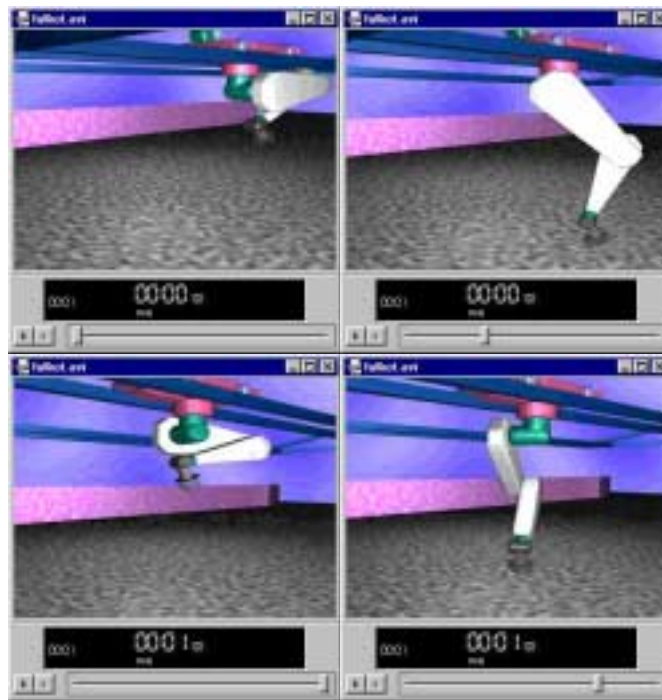


Fig. 45. Simulation sequence.

The following DK parameters have been used:

Form5 dialog box for DK parameters. It contains two columns of input fields for joint angles and a distance parameter. The left column has theta1=0, theta2=90, theta3=10, theta4=90, theta5=0, and Sx=0. The right column has theta1=180, theta2=0, theta3=340, theta4=270, theta5=360, and Sx=100. A central button labeled '>>>>' is positioned between the two columns. A 'Cancel' button is at the bottom center.

Fig. 46. DK parameters.

Some of the general geometrical and physical parameters that have been used are here (figure 47):

Generals dialog box for general parameters. It contains various input fields for mass, geometry, and material properties. The left column includes G=200, M1=25000, M2=5000, M3=2500, M4=1000, M5=4000, Lambda=25, H=20, Density=2.799, and Thick=0.5. The right column includes H=5, W=40, L=90, R=12.5, H1=20, H=5, W=15, L=120, H=5, W=11, L=50, H=5, W=5, L=15, Rtire=20 (10..50), Alpha=0 (0..45), Cx=20 (-100..100), and Cy=35 (-100..100). There are 'Compute' buttons for the right column and 'Default', 'Cancel', and 'OK' buttons at the bottom.

Fig. 47. General parameters.

The torque distributions for 3 joints, considering these inputs and a 1-second relocation move is shown in figure 48, 49 and 50. The maximum and minimum values of the torque applied are shown, the time interval varies from 0 to 1.

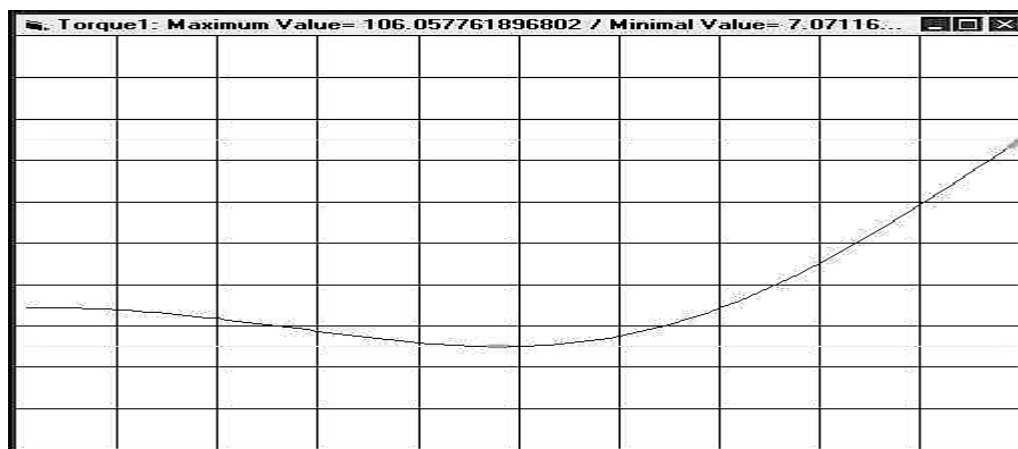


Fig. 48. Torque 1 distribution in the interval of a second.

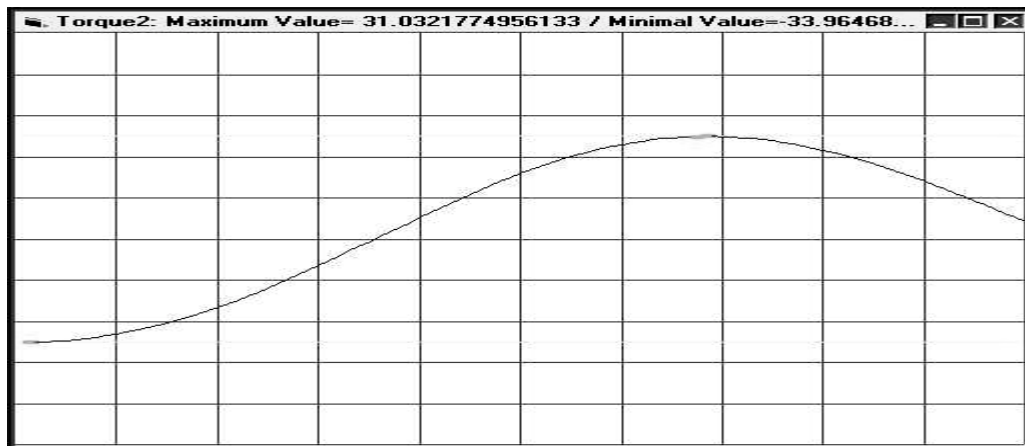


Fig. 49. Torque 2 distribution in the interval of a second.

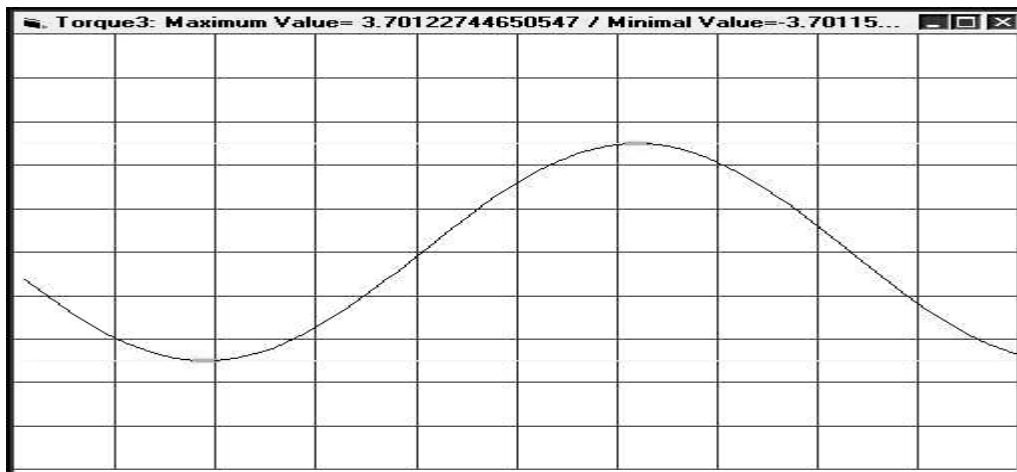


Fig. 50. Torque 3 distribution in the interval of a second.

7. Control Analysis

It is very important to have an accurate simulation and control model before having such a robot implemented. In testing and optimizing our models, we have successfully used a software package designed here at University of Bridgeport by student Mher Grigorian, presented in his paper *Design-Simulation-Control Package for a Generic 6-DOF Manipulator with a Spherical Wrist [xx]*. Although our robot is not exactly a 6 DOF manipulator, we can easily view it so if we disregard the slider, a part that will anyway have its trajectory and positions determined independently from the rest of the arm (see 3. *Direct and Inverse Kinematics Approach*).

7.1 ROBOT SOLVING

The first part of the software package, will solve most of the robot modules of equations. Though we have solved and tested our robot's equation modules with the proprietary software package, it is very important to be able to test the results through a second package.

For the direct kinematics, given the D-H parameter table, the package creates the $A_0^1 \dots A_5^6$ matrices and obtain the $T_0^1 \dots T_0^6$ transformation matrices in their symbolical form and base coordinates. For velocity kinematics, the software successfully derived the Jacobean matrix and output equations in the form

$$\dot{X} = J * \dot{Q}$$

Where:

\dot{X} = The Cartesian velocity vector,

J = The Jacobean matrix,

\dot{Q} = The joint velocity vector

The package also implements a symbolic matrix inversion routine that allows for the equations of the inverse velocity too.

Through its symbolic differentiation routines, the package is also providing the acceleration and inverse acceleration kinematics equations.

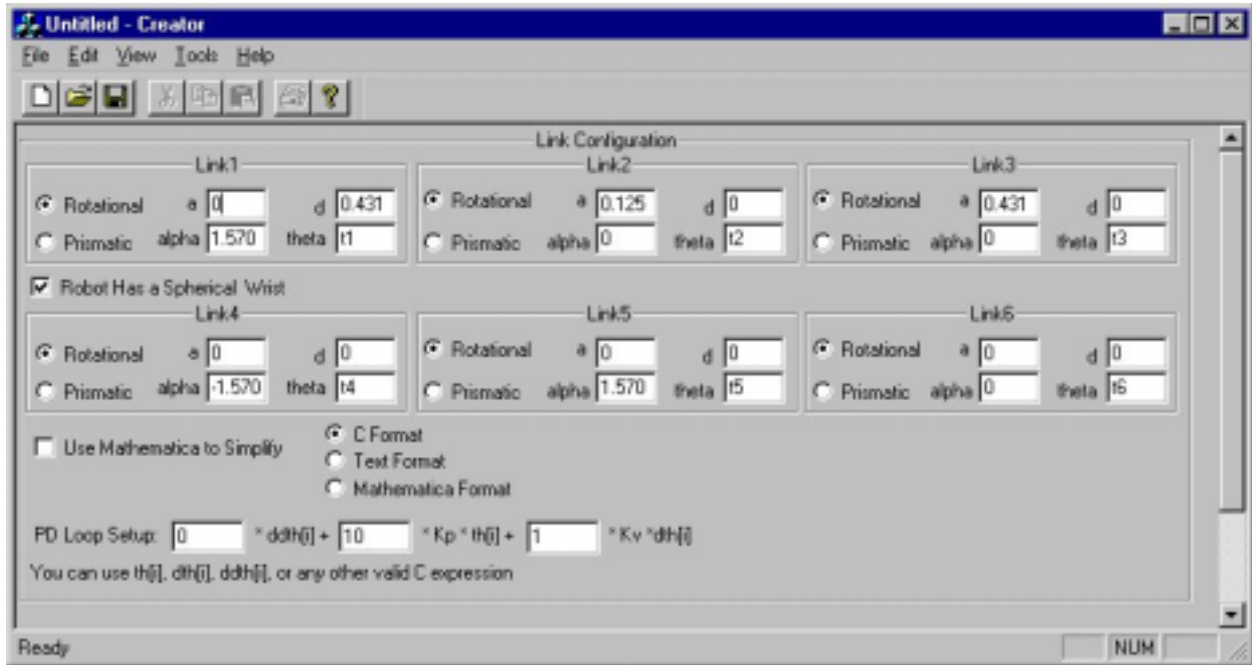


Fig 51. Input parameter window of the simulation-control package

Trajectory plotting equations are being output as well from this software package, allowing for either cubic polynomial form or constant velocity with cubic polynomial blends. We have opted for the second choice. Three time intervals can be chosen, a t_0-t_1 interval for an accelerating motion, a t_2-t_3 interval for decelerating motion and a t_1-t_2 for a linear/constant velocity period.

Given the M, G and V matrices (see 4. *Direct and Inverse Dynamics Approach*), the package outputs the dynamics and inverse dynamics equations too. A great point is that all of the equations are generated in text, C/C++ source code, or Mathematica format, thus easy to be used for further scaling.

Once we have obtained the necessary output from the package, testing in parallel with our software revealed a clear consistency.

7.2 SIMULATION AND OPTIMIZATION

The second part of the software package, also called the execution module, was of particular use for our tire changer. The package implements a local PD controller on the control function:

$$\tau = f(Q, \dot{Q}, \ddot{Q}) * \ddot{Q} + f(Q, \dot{Q}, \ddot{Q}) * K_p * e_p + f(Q, \dot{Q}, \ddot{Q}) * K_v * e_v$$

Where:

f = A function of robot joint position, velocity and acceleration vectors (note that the package allows for any mathematical function),

\ddot{Q} = The desired link acceleration vector,

K_p = The proportional gain,

K_v = The derivative gain,

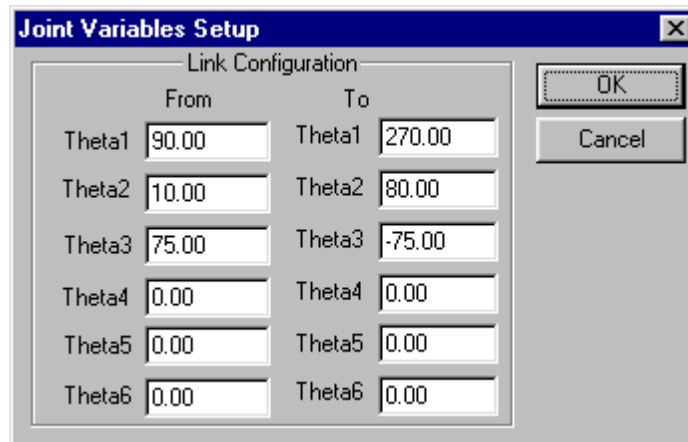
e_p = The error in joint variables vector,

e_v = The error in joint velocities vector.

The package also allows to add a PID or other feedback control functions.

Since we do not have the actual sensors to submit input to the control system, the inverse dynamics module will take their place. After providing K_p , K_v , the initial and final positions, the time interval in which the movement should be committed, the number iterations in the PD loop and the trajectory generator to be used, the package will run the control loop on points specified by the user and output graphs showing the ideal and the real trajectories of the manipulator, plus searching and optimizing the K_p and K_v values.

As an example, we run the control loop on a move similar to the fully compressed - fully extended one for which we have included the torque graphs (See 6.3), one second time limit. Note that the wrist was let aside, as it does not present much optimization interest.



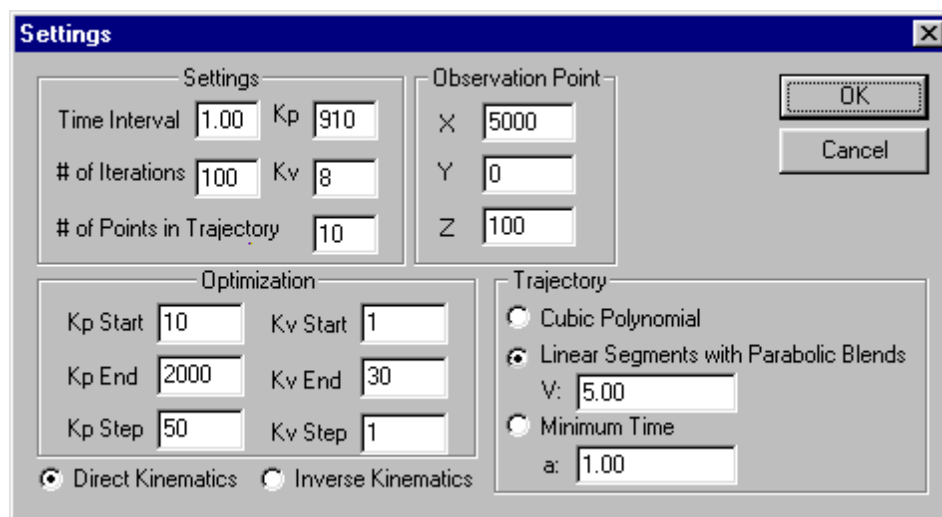
Joint Variables Setup

Link Configuration

| | From | To |
|--------|-------|---------------|
| Theta1 | 90.00 | Theta1 270.00 |
| Theta2 | 10.00 | Theta2 80.00 |
| Theta3 | 75.00 | Theta3 -75.00 |
| Theta4 | 0.00 | Theta4 0.00 |
| Theta5 | 0.00 | Theta5 0.00 |
| Theta6 | 0.00 | Theta6 0.00 |

OK Cancel

Fig 52. Setting up the thetas for the PD loop



Settings

Settings

Time Interval: 1.00 Kp: 910

of Iterations: 100 Kv: 8

of Points in Trajectory: 10

Observation Point

X: 5000

Y: 0

Z: 100

Optimization

Kp Start: 10 Kv Start: 1

Kp End: 2000 Kv End: 30

Kp Step: 50 Kv Step: 1

☒ Direct Kinematics ☐ Inverse Kinematics

Trajectory

☐ Cubic Polynomial

☒ Linear Segments with Parabolic Blends

V: 5.00

☐ Minimum Time

a: 1.00

OK Cancel

Fig 53. Additional PD data for the loop control

As output, we can see the desired thetas versus the actual ones. The package also provided the optimal K_p and K_v values, after looping on the intervals and parameters preset.

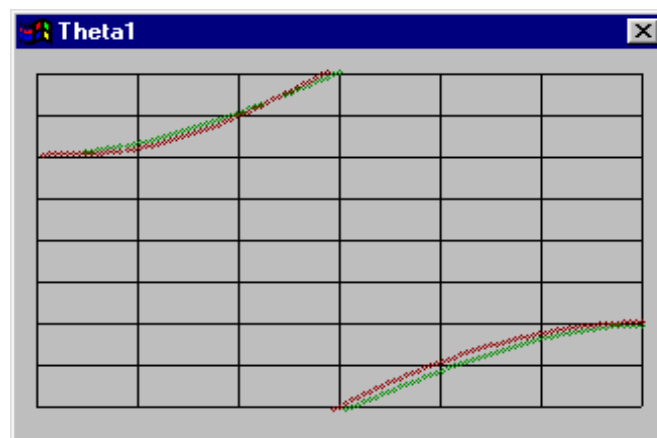


Fig 54. Theta1 (desired versus actual)

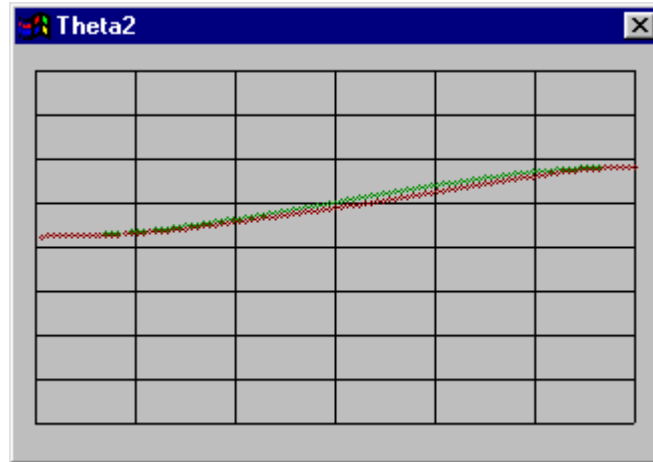


Fig 55. Theta2 (desired versus actual)

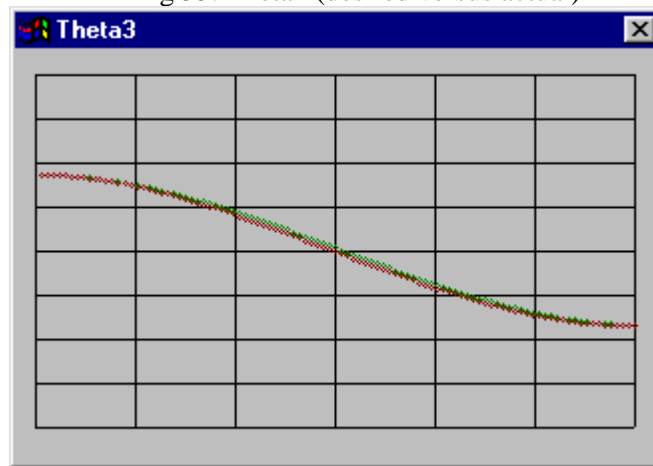


Fig 56. Theta3 (desired versus actual)

With the help of the trajectory plotting part of the program, we were able to script the output into our model and analyze the trajectories on the move. It is of major importance to have all the trajectories of the manipulator well defined, as it will be operating in a variably changing field of obstacles, any collision could not be tolerated. Figure 54 shows the trajectories of the move described above: the trajectory of the upper arm, elbow and wrist:

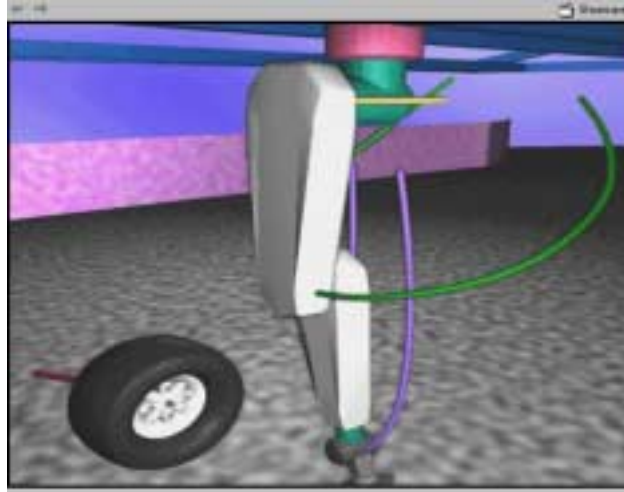


Fig 57. Plotted trajectories

The following are examples of other trajectories that have been successfully improved with the help of the package (constant speed all the time).

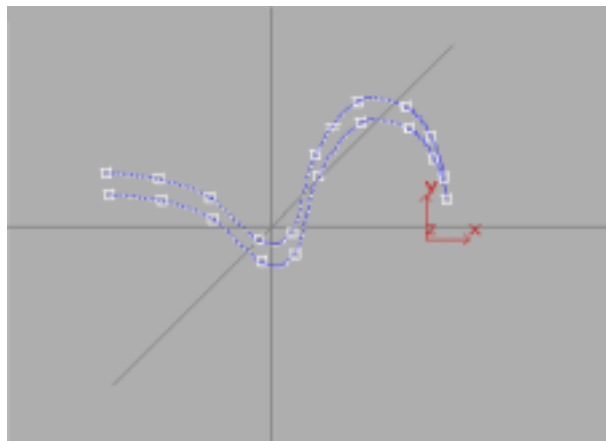


Fig 58. End Effector trajectory analysis 1

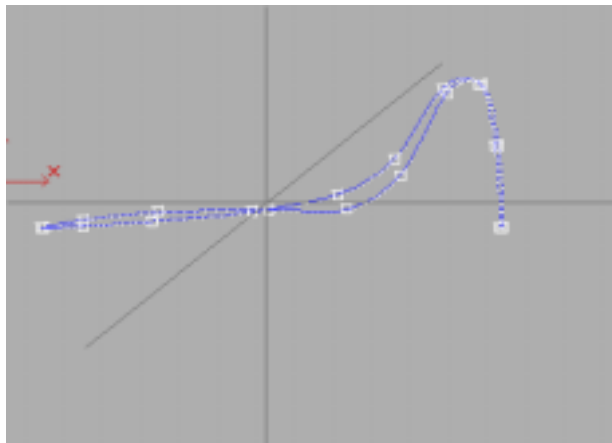


Fig 59. End Effector trajectory analysis 2

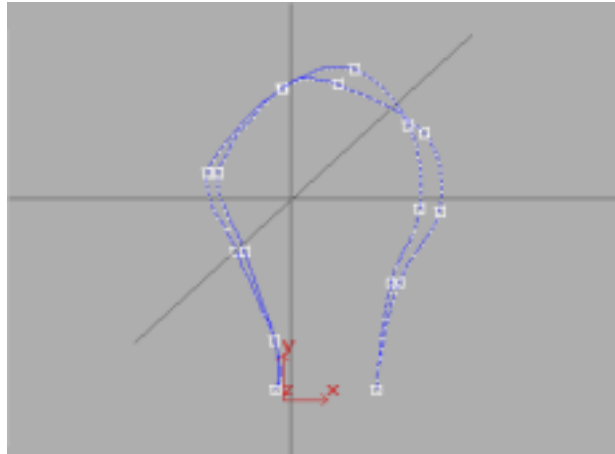


Fig 60. End Effector trajectory analysis 3

Note that most of the simulation sequences discussed here are included as AVI movies, on the demo CD of the paper. With the help of the software package, we were able to analyze and improve on all of the movement that our tire changer performs while changing a tire.

8. Conclusions

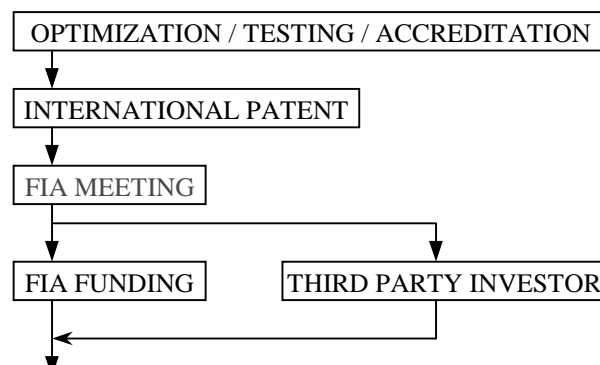
The main advantage introduced by the semi-autonomous system proposed here is the elimination of the human risks (no more team members required near a car). The five manipulators are able not only to change the tires of a car and refuel without assistance, but to obtain critical parameters of the car and interpret them in real-time.

The second advantage is the low-variance time for pit stops for any team. Once a prototype will be ready, further optimizations will allow minimization of this time (currently estimated at 10 seconds).

Future work will address the refueling manipulator and complete the integration of the entire system within the FIA restrictions.

9. From Project to Reality, Business

The project is in a stage of continuous testing and analysis and is being presented with success to various conferences and publishers. Sophisticated simulation tools are being added and used for further testing, to verify and analyze the near future manufacturing process. Once all the necessary simulation and design aspects have been exhausted, the project will have to follow a series of specific steps until it takes final shape (Figure 61).



|

Fig 61. Business Plan

9.1. PATENTING

The idea of changing the tires of a vehicle using suspended manipulator is new at the time. Although the current implementation has a very specific and limited character, it has to be protected under an international patent as future implementations could extend to more profitable consumer oriented markets. This is also an essential step in securing a trustworthy approach of any investor. Because the system will be implemented worldwide, on every Formula One race track, it is preferable to apply for an international patent.

9.2. FIA APPROACH

Unlike the design and development of most of the production robots, the case of the F1-TCR is slightly different, having as destination a field that is mainly entertaining and not productive. Formula One racing is directly controlled and supervised by Federation Internationale De L'Automobile, located in Geneva. Any safety measure, new feature, cancellation or approval needs to go through them. The organization has full executive power, which means that once the project is presented to them and they agree on its urgent necessity, the cost implied could be easily covered by funds provided by them. These funds are usually raised from competing teams and profits of the Formula One racing events.

The cost of implementing a completely functional and ready to use set of five arms, would still have to be discussed, but at a glance, a fund of a million dollars should suffice.

If FIA does not consider the implementation of the new tire changing system a necessity, no further steps are considered and the project remains in a patented stage.

Indianapolis 500 would be a second choice to work with. However, Indianapolis 500 racing rules are significantly less restrictive, there are fewer standards and safety was never really a big concern. It is still possible that a fast tire changer that maintains the same constant time during pits for every team would interest them, this remains to be discussed in the small eventuality that FIA rejects the system.

9.3. MANUFACTURER APPROACH

For testing and manufacturing on a production scale, there are various robotics companies on the market that are available and willing to provide their services if funded, or not funded at all if they find ideas profitable. Opening a robot manufacturing company for the sole purpose of having a production line of F1-TCR robots would not be simple at all, the start up capital would be difficult to obtain and the amortization costs risky.

We have analyzed most of the major consumer robot manufacturers: ActivMedia Robotics, Adept Technology Inc., American Robot Corporation, Angelus Research, Arrick Robotics, CRS Robotics, Cybermotion, Diversified Enterprises, FANUC Robotics, IS Robotics, K-Team SA, Mekatronix, Motoman, Nimbl, Nomadic Technologies, Real World Interface, Rixan Associates Inc., Sankyo Robotics, Seiko, Terra Aerospace Corp. Ublige Software and Robotics, Ventax Robot Inc.. Our focus is on CRS Robotics, FANUC Robotics and Motoman. These are the main companies that have considerable experience in constructing solid, fast and accurate articulated industrial scale robots.

9.3.1. *CRS Robotics*

CRS (<http://www.crsrobotics.com/>) already offers related manipulators like the T475 and F3t Track Robots. They are prepared for working on sliders, at great speeds and precision (speeds between 0.01 and 1.0 m/s with repeatability of 0.08 mm, see web site for full specs), and are ready for industrial scale tasks. The work with CRS would emphasize on making the manipulators lighter and with higher payloads, and should be minimal.



Fig 62. CRS T475 Track Robot

9.3.2. *FANUC Robotics*

FANUC (<http://www.fanucrobotics.com/>) offers a variety of robots that support high payloads, have a slim construction and are also fast, like the M-16L (16kg payload capacity, ± 0.003 m repeatability, axes speed up to 450° per second, see web site for full specs). Working with FANUC would focus on making the manipulators lighter and installable on tracks.

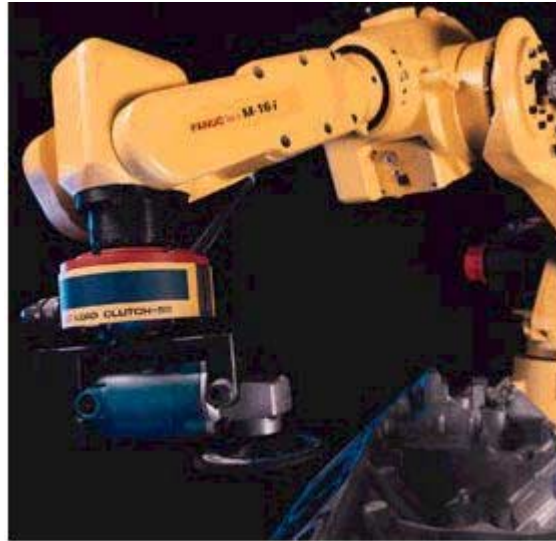


Fig 63. FANUC M-16L Robot

9.3.3. Motoman

The Swedish company Motoman (<http://www.motoman.se/>) robots are some of the strongest production manipulators (SK series, lifting up to 300Kg, ± 0.5 mm, please see web site for full specs), fast, with thin arm structure and easy to customize. However, they have very heavy links (hundreds of kilograms), and lowering their weights to values of tens of kilograms might be difficult.



Fig 64. Motoman SK16 Robot

8.4 MANUFACTURING / PRODUCTION LINE SETUP

Once the manufacturer has been chosen, we expect a completion period of less than 6 months. In this time, a full production line will be setup, allowing manufacturing of full manipulator sets in matter of days. The manipulators resulted from this first production line, will undergo vast testing and optimization procedures on the tracks, and other 3 months are estimated to finalize the production line

and reach a complete, final version of the system. Another month will be needed to have the new tire changing system installed on all the tracks that are used in Formula One racing. Replacement parts and other supplies will be available and installed immediately upon request.

Once the production line is rolling, we approximate the cost of a full tire changing system around \$200,000. On track installation, personnel training and qualification and technical assistance will be offered as needed. Our royalties as inventors are 5% of sales. In the case of future applications based on our patent, the royalties remain the same, plus a "per license" cost will be instated.

References

- [1] Spong, W. Mark, "*Robot Dynamics and Control*", John Wiley, 1989
- [2] McKerrow, Phillip John, "*Introduction to Robotics*", Addison Wesley, 1991
- [3] Dekhil, Mohamed, and Sobh, Tarek M., and Henderson, Thomas C., and Sabbavarapu, Anil, and Mecklenburg, Robert, "*Robot Manipulator Prototyping (Complete Design Review)*", University of Utah, 1994
- [4] Nakamura, Yoshihiko, "*Advanced Robotics - Redundancy and Optimization*", Addison-Wesley, 1991
- [5] Marris, Andrew W., and Stoneking, Charles E., "*Advanced Dynamics*", McGraw-Hill, 1967
- [6] Christie, Dan Edwin, "*Intermediate College Mechanics*", McGraw-Hill, 1952
- [7] De Wit, Charlos Canudas, and Siciliano, Bruno, and Bastin, Georges, "*Theory of Robot Control*", Springer-Verlag London, 1996
- [8] Sobh, Tarek M., Dekhil, Henderson, Thomas, C. and Sabbavarapu, A. "*Prototyping a Three-link Robot Manipulator*," Presented in the Second World Automation Congress, Sixth International Symposium on Robotics and Manufacturing (ISRAM 96), Montpellier, France, May 1996
- [9] Herrea-Beneru, L. ,Mu, E. ,Cain, J. T., "*Symbolic Computation of Robot Manipulator Kinematics*", Department of Electrical Engineering, University of Pittsburgh
- [10] Rieseler, H., Wahl, F. M., "*Fast symbolic computation of the inverse kinematics of robots*", Institute for Robotics and computer control, Technical University of Braunschweig
- [11] Dekhil, M., Sobh, T. M., Henderson, T. C. and Mecklenburg, R. "*UPE: Utah Prototyping Environment for Robot Manipulators*". In proceedings of the IEEE International Conference on Robotics and Automation, Nagoya, Japan, May 1995
- [12] Schalkoff, R. J. "*Digital Image Processing and Computer Vision*", John Wiley and Sons, Inc., 1989
- [13] J. Hervé, P. Cucka and R. Sharma, "*Qualitative Visual Control of a Robot Manipulator*". In Proceedings of the DARPA Image Understanding Workshop, September 1990
- [14] M. J. Banks and E. Cohen, "*Realtime B-Spline Curves from Interactively Sketched Data*," Proceedings of the 1990 Symposium on Interactive 3-D graphics, ACM, March 1990

- [15] J. A. Thingvold and E. Cohen, "*Physical Modeling with B-Spline Surfaces for Interactive Design and Animation*," Proceedings of the 1990 Symposium on Interactive 3-D graphics, ACM, March 1990
- [16] Y. Li and W. M. Wonham, "*Controllability and Observability in the State-Feedback Control of Discrete-Event Systems*", Proc. Conf. on Decision and Control, 1988
- [17] Benedetti, R., and Risler, J. J. "*In Real Algebraic and Semi-algebraic Sets*" (1990), Hermann, pp. 8-19
- [18] P. K. Allen, "*Robotic Object Recognition Using Vision and Touch*", 1987. Kluwer Academic Publishers, Norwell, MA
- [19] Craig, John J., "*Introduction to Robotics. Mechanics and Control. Second Edition*", 1989, Addison Wesley